The first crystal structure of an RNA racemate

Wojciech Rypniewski,[a,b]‡ Marco Vallazza,[c]‡ Markus Perbandt,[d] Sven Klussmann,[e] Lawrence J. DeLucas,[f] Christian Betzel[g] and Volker A. Erdmann[c]*

[a]Institute of Bioorganic Chemistry, Polish Academy of Sciences, Poland, [b]Institute of Biochemistry and Molecular Biology I, University Hospital Hamburg-Eppendorf, Germany, [c]Institute of Biology, Chemistry and Pharmacy, Free University of Berlin, Germany, [d]Department of Biochemistry and Molecular Biology, Hamburg University, Germany, [e]NOXXON Pharma AG, Germany, [f]Center for Macromolecular Crystallography, University of Alabama, USA, and [g]Institute of Biochemistry and Molecular Biology, Hamburg University, Germany

‡ These authors contributed equally to this work.

Correspondence e-mail: erdmann@chemie.fu-berlin.de

The racemate of the RNA duplex r(CUGGGCGG)·r(CCGCCUGG) from *Thermus flavus* 5S rRNA has been crystallized and examined by X-ray crystallography. The space group is $P\bar{1}$ with approximate unit-cell parameters $a = 26.5$, $b = 38.0$, $c = 45.4$ Å, $\alpha = 113.1$, $\beta = 100.5$, $\gamma = 93.3°$. The structure was solved by molecular replacement. There are four RNA duplexes in the unit cell. The crystal lattice consists of columns of RNA duplexes. The duplexes are stacked end-to-end and are stabilized by intermolecular base-stacking interactions. Within each column the L-duplexes and D-duplexes are stacked alternately. Every other duplex in each stack has two alternative conformations, approximately equally occupied, corresponding to molecules oriented in opposite directions. Neighbouring columns are related by the crystallographic centre of symmetry. The unit cell also contains approximately 250 ordered water molecules and six ordered calcium ions. A glycerol molecule is visible in the minor groove interacting with a guanosine residue.

1. Introduction

In recent years, RNA has revealed a multifaceted nature, extending well beyond its traditionally assigned function in the machinery of protein synthesis. Approximately half of nuclear DNA is transcribed in higher organisms, but only a few percent of that is translated (see review by Szymanski *et al.*, 2005). Thus, a large part of the genome is expressed in the form of RNA. Vast quantities of non-coding RNA molecules are produced and many of them have been demonstrated to affect vital processes such as regulation of protein synthesis (Zhanybekova *et al.*, 1996), gene silencing (Sleutels *et al.*, 2002), alternative gene splicing, polyadenylation, repair of DNA damage, heat-shock response, sex differentiation, regulation of neural functions, X-chromosome inactivation, regulation of iron uptake, control of steroid receptors, early postnatal development (Szymanski *et al.*, 2003), carcinogenesis (Thrash-Bingham & Tartof, 1999), cell cycle (Watanabe *et al.*, 1997), antiviral defences (Kimura *et al.*, 2001), oxidative stress response (Altuvia *et al.*, 1997) and cell secretion (Zwieb & Larsen, 1997). Certainly, many more functions of RNA still await discovery.

These recent discoveries have opened up a vast new field of study. The revelation of the functional diversity of RNA points to the correspondingly rich structure–function relationship in RNA, rivalling that observed in proteins. Yet, the studies of RNA structure are certainly less advanced than in the case of proteins. As of 31 January 2006, the RCSB/NDB database contained 444 RNA structures compared with almost 32 000 protein structures.

659

Table 1
Summary of the X-ray data and statistics.

Values in parentheses are for the high-resolution bin: 1.37–1.35 Å for DLE-S, 1.42–1.40 Å for DLE-G, 1.42–1.40 Å for DLE-ctrl1, 1.32–1.30 Å for DLE-ctrl2, 1.32–1.30 Å for DLE-ctrl3 and 1.63–1.60 Å for DLE-ctrl4.

Crystal name	DLE-S	DLE-G	DLE-ctrl1	DLE-crtl2	DLE-ctrl3	DLE-ctrl4
Where crystallized	Space	Ground	Ground	Ground	Ground	Ground
Beamline	BW7A	X13	X13	X13	X13	X13
Wavelength (Å)	0.980	0.802	0.803	0.803	0.801	0.805
Space group	$P\bar{1}$	$P\bar{1}$	$P\bar{1}$	$P\bar{1}$	$P\bar{1}$	$P\bar{1}$
Unit-cell parameters						
a (Å)	26.9	26.3	26.4	26.1	26.3	26.7
b (Å)	38.2	38.1	38.0	37.9	37.7	37.9
c (Å)	45.9	45.4	45.20	45.3	45.1	45.4
α (°)	112.3	113.8	113.2	113.5	112.9	122.6
β (°)	101.6	99.7	100.3	100.0	100.7	100.9
γ (°)	92.2	93.9	93.5	93.6	93.0	93.3
R_{merge}†	0.031 (0.580)	0.072 (0.444)	0.065 (0.427)	0.084 (0.313)	0.056 (0.521)	0.081 (0.497)
Mosaicity (°)	0.6	0.8	0.6	0.7	0.8	1.2
Resolution range (Å)	10.0–1.35	20.0–1.40	20.0–1.40	20.0–1.30	20.0–1.30	20.0–1.60
Completeness (%)	95 (92)	97 (94)	97 (95)	96 (95)	97 (95)	98 (97)
No. of raw data	397975	189735	191903	235021	564094	331039
No. of unique reflections	34434	29605	28908	36127	37268	20724
$I/\sigma(I)$	37 (2.3)	12 (2)	14 (2.5)	6 (3.3)	19 (3.1)	17 (2.9)
R_{work}	0.241	0.245	0.252	0.264	0.239	0.231
R_{free}	0.270	0.332	0.318	0.295	0.258	0.310
No. of RNA atoms	680	680	680	680	680	680
No. of water molecules	281	251	225	214	258	248
No. of Ca²⁺ sites	6	6	6	6	6	6
No. of glycerol molecules	1	0	1	1	1	1

† $R_{merge} = \sum |I - \langle I \rangle| / \sum I$, where $\langle I \rangle$ is the average intensity for a given measurement and the summation is over all measurements.

RNA oligonucleotides with high affinity for a wide range of biological target molecules can be identified by an *in vitro* evolutionary process. These molecules are termed aptamers. They have also been described as natural elements that can regulate gene expression. Among aptamers, those known as a Spiegelmers are promising tools in biotechnology and molecular medicine. Spiegelmers consist of ʟ-ribonucleotides and are invulnerable to natural degradation processes. This work is part of the project aimed at studying mirror-image RNA and their interactions with natural RNA. Here, we report the first crystal structure of an RNA racemate.

2. Materials and methods

2.1. Crystallization and data collection

The oligoribonucleotides E3-79 (5′-CUGGGCGG-3′) and E3-90 (5′-CCGCCUGG-3′) have been chemically synthesized in the ᴅ- and ʟ-configuration and purified as described previously (Perbandt *et al.*, 2001; Vallazza *et al.*, 2004). The ᴅ-RNA helix and the ʟ-RNA helix were separately annealed (Perbandt *et al.*, 2001). Equal amounts of the ᴅ- and ʟ-helix were mixed to a final racemate concentration of 0.25 mₘ. Of the commercial and self-developed screening conditions (Nucleic Acid Mini Screens, Crystal Screens 1 and 2, Grid Screen Ammonium Sulfate and Natrix from Hampton Research; JBScreen 6 from Jena Bioscience; RNA-MPD Screen from Vallazza *et al.*, 2001), 24 were found to give crystals. The crystals were grown in the laboratory and under microgravity. The space crystallization was performed on the

International Space Station (ISS) in the High Density Protein Crystal Growth (HDPCG) apparatus, as previously described by Vallazza *et al.* (2004), during the mission ISS-8A for a period of 67 d from 10 April to 17 June 2002. Complete data sets could be collected from crystals grown in drops containing 0.25 mₘ RNA, 7%(v/v) PEG 400, 0.1 *M* CaCl₂, 0.05 *M* Na HEPES pH 7.5 at 295 K and which were cryoprotected with 7.5%(v/v) glycerol in 24%(v/v) PEG 400, 0.17 *M* CaCl₂, 0.085 *M* Na HEPES pH 7.5. X-ray diffraction data were collected from crystals cryocooled to 100 K at the DESY/HASYLAB synchrotron in Hamburg; one data set was obtained on the EMBL beamline BW7A and the other data sets on the X13 Consortium beamline. One data set was collected from a space-grown crystal (DLE3-S) followed by five data sets from the ground crystallization experiments (DLE3-G and DLE3-ctrl1–DLE-ctrl4), as summarized in Table 1.

2.2. Structure solution and crystallographic refinement

The structures were solved by molecular replacement using the program *AMoRe* (Navaza, 2001; Collaborative Computational Project, Number 4, 1994) using as a search model the previously solved structure of the E domain of 5S rRNA (Perbandt *et al.*, 2001) and its mirror image. The atomic coordinates were subsequently refined using the program *REFMAC*5 (Murshudov *et al.*, 1997) and the solvent molecules were inserted using the program *ARP/wARP* (Lamzin & Wilson, 1993) with automatic determination of statistically significant density levels for inclusion of new water molecules.

The calculated values were in the range 3.2–3.6 r.m.s. level in the $F_o - F_c$ map. Refinement was initially carried out in space group $P1$ without imposing any symmetry between the molecules and then in space group $P\bar{1}$ after a suitable reduction of the real-space asymmetric unit. The reduction consisted of selecting the appropriate half of the RNA chains, any ligands and ions, but the water structure was rebuilt *ab initio*. Occupancy factors of calcium ions were adjusted in the cases where refinement of atomic coordinates and isotropic temperature factors was insufficient to reduce the residual $F_o - F_c$ difference density below the 3 r.m.s. level and there the atomic temperature factors were unreasonably high compared with the surrounding atoms. The occupancies were then adjusted manually and the model was further refined using *REFMAC*5 until the difference density was within the 3 r.m.s. level and the atomic temperature factors of the atoms in question were comparable to those of the surrounding atoms.
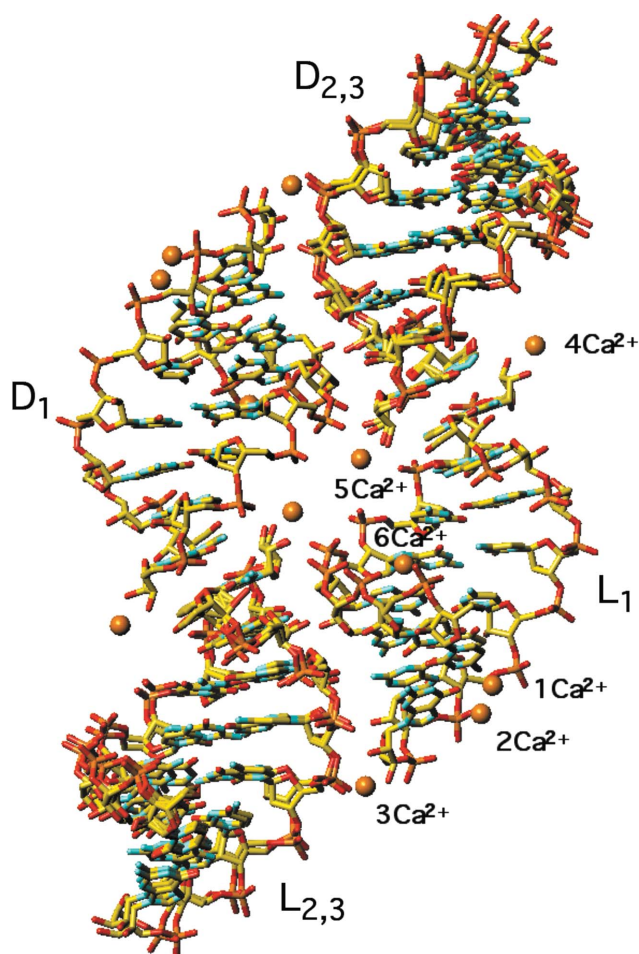
Figure 1
The content of the DLE-ctrl3 unit cell. The L- and D-duplexes are related by the centre of symmetry in the middle of the picture. The columns of RNA duplexes are oriented vertically in this view. L-Duplexes and D-duplexes are stacked alternately in an end-to-end manner. Every other duplex (labelled $L_{2,3}$ and $D_{2,3}$) in each column is disordered as described in the text. The six unique calcium ions are shown as labelled spheres; the symmetry-related ions are not labelled. Water molecules and glycerol have been omitted for clarity.

Calcium ions were distinguished from solvent water molecules by coordination distances and higher electron density. Occupancy factors of the alternative positions in the disordered duplexes were set to 0.5 and subsequently verified against the $F_o - F_c$ maps. The alternative positions appeared to be equally occupied in all the examined structures. The other atoms, RNA and solvent water, had occupancy factors set to 1.0. Independently refined models based on the six analysed crystals were used to derive average values of the helical parameters and the associated standard deviations.

3. Results

3.1. The overall structure

The racemate of the RNA duplex r(CUGGGCGG)·r(CCGCCUGG), from *Thermus flavus* 5S rRNA has been crystallized and examined by X-ray crystallography. Six crystals grown under comparable conditions have been analysed (Table 1). The packing of the molecules and the unit-cell parameters are similar in all the examined crystal structures. In each case the RNA enantiomers are arranged in a centrosymmetric crystal lattice. The are four RNA duplexes in the $P\bar{1}$ unit cell. The crystal lattice consists of columns of RNA duplexes. The duplexes are stacked end-to-end and are stabilized by intermolecular base-stacking interactions. Within each column, the L-duplexes and D-duplexes are stacked alternately. Neighbouring columns are related by the crystallographic centre of symmetry. Every other duplex in each column has two alternative conformations corresponding to molecules oriented in opposite directions. The two conformations are closely matched at the helical ends, where the duplex is quasi-palindromic, and they are most different in the middle where the electron density of CC·GG overlaps with its reverse. The alternative positions appear to be equally occupied. Thus, one column of RNA molecules consists of D-duplexes and disordered L-duplexes stacked alternately. The neighbouring symmetry-related column consists of L-duplexes and disordered D-duplexes (Fig. 1). In the observed end-to-end RNA-stacking interactions the 3′-ends are close to the 5′-ends, similar to the commonly observed stacking of oligonucleotides of the same handedness. In the racemic stacking, however, the sugar-phosphate backbones of stacked oligonucleotides trace a zigzag pattern along the resulting pseudo-infinite columns, owing to the opposite helical twist of the consecutive fragments. The asymmetric unit also contains ~250 ordered water molecules hydrating the RNA and six calcium ions. These features are common to all the examined structures. In five of the six experiments glycerol was used as cryoprotectant during the X-ray data collection and one ordered glycerol molecule is visible in these structures.

3.2. Helical parameters

The helical parameters of the ordered RNA duplex are summarized in Table 2. The other duplex present in the crystal lattice is disordered and has not been included in the comparison. A comparison is also given with the previously

Table 2
Helical parameters for the racemic RNA model and the corresponding L-RNA (Vallazza *et al.*, 2004) and D-RNA (Perbandt *et al.*, 2001).

The parameters were calculated with the program 3*DNA* (Lu & Olson, 2003).

(*a*) Overall helical parameters.

	Twist (°)	Rise (Å)	Roll (°)	*x* displacement (Å)	Prop. (°)
L+D-RNA†	32.1	2.7	7.2	−4.2	−10.0
L-RNA‡	−31.9	2.7	5.3	−5.5	−8.9
D-RNA	32.9	2.6	6.7	−5.3	−10.8
t-RNA	33.2	2.5	5.2	−4.4	−14.2

(*b*) Local helical parameters.

Values in parentheses are standard deviations based on a comparison of the six racemic crystal structures.

	Twist (°)			Rise (Å)			*x* displacement (Å)		
	L+D-RNA	L-RNA	D-RNA	L+D-RNA	L-RNA	D-RNA	L+D-RNA	L-RNA	D-RNA
C79–G97									
	36.9 (0.3)	−29.0	31.4	3.0 (0.1)	3.3	3.2	−2.3 (0.1)	−4.9	−3.8
U80–G96									
	23.8 (1.0)	−38.8	43.5	1.5 (0.1)	1.8	1.9	−9.8 (0.5)	−8.0	−5.5
G81–U95									
	35.2 (0.5)	−27.0	29.9	3.3 (0.1)	3.0	2.9	−2.7 (0.1)	−5.7	−5.4
G82–C94									
	33.4 (0.4)	−32.7	29.4	2.7 (0.1)	2.5	2.4	−4.2 (0.1)	−6.3	−6.8
G83–C93									
	34.5 (0.3)	−29.4	28.1	3.0 (0.1)	3.3	3.2	−2.9 (0.1)	−2.6	−3.4
C84–G92									
	35.2 (0.5)	−33.8	35.2	2.3 (0.1)	2.3	1.7	−4.8 (0.2)	−7.7	−7.6
G85–C91									
	35.5 (0.5)	32.2	33.0	2.9 (0.0)	3.5	2.7	−3.1 (0.1)	−4.8	−4.8
G86–C90									

† Based on average values for duplex L_1 in the six analysed structures. ‡ Average parameters for the two L-RNA duplexes in the crystal asymmetric unit.
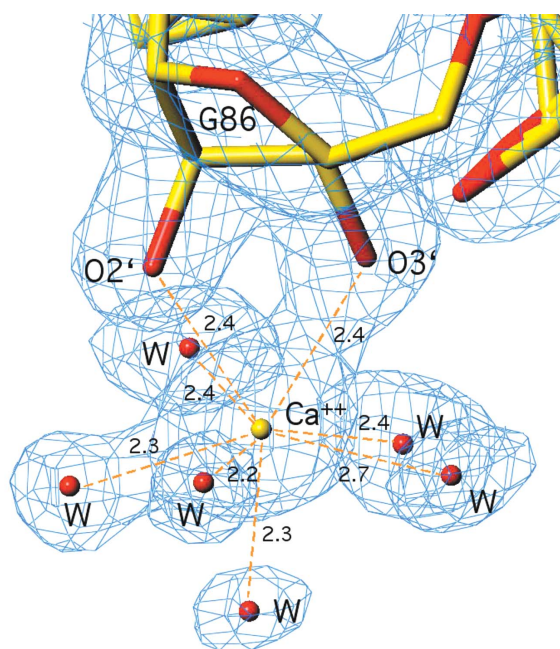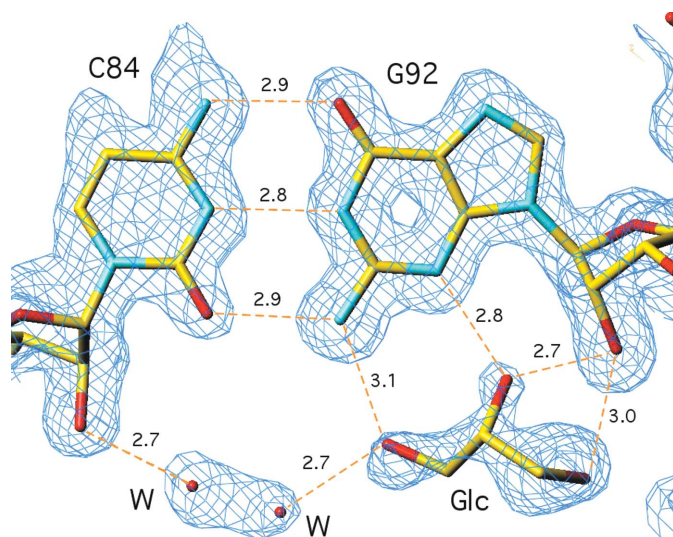

Figure 2
A hydrated calcium ion capping the terminal sugar moiety of G86. The contours correspond to the $2F_o − F_c$ electron density at one r.m.s. level. Water molecules are labelled W.

analysed crystal structures of the corresponding L-RNA (Vallazza *et al.*, 2004) and D-RNA (Perbandt *et al.*, 2001). The overall duplex structure of this crystal form is similar to the other two crystal structures used in the comparison. The RNA duplexes adopt the A-conformation with an average helical twist of 32° or 11 residues per helical turn. All the ribose rings are in the C3′-*exo* puckering conformations. All the α backbone torsion angles are in the g^+ conformation and all the γ torsion angles are in the g^- conformation. The large value of x displacement of 10 Å is associated with the U·G/G·U step. The two G residues that pair with the U residues form the characteristic 'cross-strand G-stack' previously observed by Perbandt *et al.* (2001). No wobble-like conformation is observed for C84·G92 base pairing. This is similar to the L-RNA structure reported by Vallazza *et al.* (2004) and different from the structure reported by Perbandt *et al.* (2001), who reported non-Watson–Crick base pairing between these residues.

3.3. Hydration and ions

More than 200 ordered water molecules are distributed around the two duplexes in the unit cell, together with six calcium ions and a glycerol molecule in the crystals where glycerol was used for cryoprotection. The differences in the

Figure 3
A glycerol molecule (Glc) bound to G92, on the minor-groove side of DLE-ctrl3. The contours correspond to the $2F_o - F_c$ electron density at one r.m.s. level. Positions labelled W are partially ordered water molecules occupying alternative sites.

numbers of ordered water molecules between the different structures are related to the X-ray data quality, as evidenced by statistics, and the resolution of the data (Table 1). The well ordered water molecules in the vicinity of the RNA occupy similar positions in the different crystals. Differences appear only in regions of partially disordered solvent density. Approximately half of the observed water molecules are located in the major groove and the rest are in the minor groove or along the sugar-phosphate backbone. Two of the calcium ions are associated with the outer side of the sugar-phosphate backbone, one has been found in the major groove and three calcium ions cap the sugar moieties of the terminal residues: G86 and G97 of the ordered duplex and G86/G97 of the disordered duplex (Fig. 2). Each Ca ion has between six and eight ordered ligands. The three ions interacting with *cis*-diols of the terminal sugar moieties have similar coordination: five water molecules and the ion are roughly coplanar, with the sixth water on one side of the plane and the two diols on the other side. The glycerol molecule is located on the minor-groove side of G92 and close to residues 80U/91C and G85/G96 of the disordered duplex (Fig. 3). One of the primary hydroxyl groups is a hydrogen-bond acceptor from the *exo*-NH$_2$ group of the G92 (hydrogen-bonding distance 3 Å). The secondary hydroxyl group of the glycerol molecule is a hydrogen-bond donor for the N3 atom of the G92 (2.8 Å) and probably a hydrogen-bond acceptor from the O2′ (2.7 Å). The other primary hydroxyl is within hydrogen-bonding distance to the O2′ of the same residue (3.1 Å) and N2 G96 and O2 C91 of the neighbouring disordered duplex. In the model DLE-G, based on the structure that did not contain glycerol, the places of the two glycerol primary hydroxyl groups are occupied by water molecules. There is only a weak water peak in the place corresponding to the secondary hydroxyl.

3.4. Space and ground data

There is only one data set from a space-grown crystal; therefore, it is difficult to make conclusive comparisons with earth-grown crystals. In terms of crystal mosaicity, the space crystal was as good (0.6°) as the best of the examined ground crystal, although the mosaicity is generally high. In terms of merging statistics, the space data are also as good or somewhat better than the best of the ground data. Many earth-grown crystals were discarded as unsuitable for diffraction experiments: proportionately more than in the case of space crystals.

4. Discussion

There are only a few crystallographic studies of biological molecules cocrystallized with their enantiomers (Zawadzke & Berg, 1993; Doi *et al.*, 1993; Toniolo *et al.*, 1994). This is the first structure of an RNA racemate. Centrosymmetric structures are common in 'small-molecule' crystallography but quite rare, for natural reasons, in the case of biological molecules. According to Kitaigorodsky (1958), 'centrosymmetric molecules are not expected to crystallize in non-centrosymmetric space groups' and his postulate is frequently confirmed experimentally. It is interesting to observe that also in the case of the racemate, the enantiomers preferentially assemble in one crystal lattice rather than crystallize separately. The commonly observed end-to-end stacking of oligomers in the crystal lattice to form pseudo-infinite columns also occurs here, but the L- and D-molecules stack alternately. This preferential interaction of different enantiomers over molecules of the same type may have useful implications for the possible use of mirror-image RNA aptamers.

It is likely that the base pairing of C84 with G92 is sensitive to pH. The unusual 'wobble' conformation occurred in the crystal form grown in pH 6.5, whereas the present structure and that reported by Vallazza *et al.* (2004) that has standard C·G base pairing was obtained at pH 7.5.

There are few published examples of Ca ions binding the *cis*-diol of terminal sugar moieties of RNA fragments (Xiong & Sundaralingam, 2000; Minasov *et al.*, 2000; Deng *et al.*, 2001). This is surprising because according to 'small-molecule' X-ray and IR spectroscopic studies of sugar–metal complexes the bidentate coordination of metal by neighbouring diol fragments is the most common in sugar complexes with *s*-metal cations (Alekseev *et al.*, 1998).

The binding of glycerol to a guanosine residue from the side of the minor groove provides insight into the issue of RNA hydration and dehydration in the presence of small ligands, especially alcohols (Adamiak *et al.*, 2001). The dehydration is effected by the ligand hydroxyl groups displacing the water molecules that interact specifically in the minor groove stabilizing the RNA duplex. In this case, the glycerol molecule displaced two well ordered water molecules. The interaction of the glycerol with the guanine residue is similar to the interaction of 2-methyl-2,4-pentanediol (MPD) with the RNA structure reported by Adamiak and coworkers (2001). In both structures the hydroxyl group of the alcohol is a hydrogen-

bond acceptor from the *exo*-amino functions of guanosine residues.

References

Adamiak, D. A., Rypniewski, W. R., Milecki, J. & Adamiak, R. W. (2001). *Nucleic Acids Res.* **29**, 4144–4153.

Alekseev, Yu. E., Garnovskii, A. D. & Zhdanov, Yu. A. (1998). *Russ. Chem. Rev.* **67**, 649–669.

Altuvia, S., Weinstein-Fischer, D., Zhang, A., Postow, L. & Storz, G. (1997). *Cell*, **90**, 43–53.

Collaborative Computational Project, Number 4 (1994). *Acta Cryst.* D**50**, 760–763.

Deng, J., Xiong, Y. & Sundaralingam, M. (2001). *Proc. Natl Acad. Sci. USA*, **98**, 13665–13670.

Doi, M., Inoue, M., Tomoo, K., Ishida, T., Ueda, Y., Akagi, M. & Urate, H. (1993). *J. Am. Chem. Soc.* **115**, 10432–10433.

Kimura, R. H., Choudary, P. V., Stone, K. K. & Schmid, C. W. (2001). *Cell Stress Chaperones*, **6**, 263–272.

Kitaigorodsky, A. (1958). *Sov. Phys. Crystallogr.* **3**, 393.

Lamzin, V. S. & Wilson, K. S. (1993). *Acta Cryst.* D**49**, 129–147.

Lu, X.-J. & Olson, W. K. (2003). *Nucleic Acids. Res.* **31**, 5108–5121.

Minasov, G., Matulic-Adamic, J., Wilds, C. J., Haeberli, P., Usman, N., Biegelman, L. & Egli, M. (2000). *RNA*, **6**, 1516–1528.

Murshudov, G. N., Vagin, A. A. & Dodson, E. J. (1997). *Acta Cryst.* D**53**, 240–255.

Navaza, J. (2001). *Acta Cryst.* D**57**, 1367–1372.

Perbandt, M., Vallazza, M., Lippmann, C., Betzel, C. & Erdmann, V. A. (2001). *Acta Cryst.* D**57**, 219–224.

Sleutels, F., Zwart, R. & Barlow, D. P. (2002). *Nature (London)*, **415**, 810–813.

Szymanski, M., Barciszewska, M. Z., Erdmann, V. A. & Barciszewski, J. (2005). *Biochim. Biophys. Acta*, **1756**, 65–75.

Szymanski, M., Erdmann, V. A. & Barciszewski, J. (2003). *Nucleic Acids Res.* **31**, 429–431.

Thrash-Bingham, C. A. & Tartof, K. D. (1999). *J. Natl Cancer Inst.* **91**, 143–151.

Toniolo, C., Peggion, C., Crisma, M., Formaggio, F., Shui, X. & Eggleston, D. S. (1994). *Struct. Biol.* **1**, 908–913.

Vallazza, M., Perbandt, M., Klussman, S., Rypniewski, W., Einspahr, H. M., Erdmann, V. A. & Betzel, C. (2004). *Acta Cryst.* D**60**, 1–7.

Vallazza, M., Senge, A., Lippmann, C., Perbandt, M., Betzel, C. & Erdmann, V. A. (2001). *J. Cryst. Growth*, **232**, 340–352.

Watanabe, T., Sugiura, M. & Sugita, M. (1997). *FEBS Lett.* **416**, 302–306.

Xiong, Y & Sundaralingam, M. (2000). *RNA*, **6**, 1316–1324.

Zawadzke, L. E. & Berg, J. M. (1993). *Proteins*, **16**, 301–305.

Zhanybekova, S. Sh., Polimbetova, N. S., Nabisbekov, N. O. & Iskakov, B. K. (1996). *Biokhimiia*, **61**, 862–870.

Zwieb, C. & Larsen, N. (1997). *Nucleic Acids Res.* **25**, 107–108.